

Mesoporous Silica Nanoparticles/Hydroxyapatite Composite Coated Implants to Locally Inhibit Osteoclastic Activity

Min Zhu,^{†,‡} Yufang Zhu,[‡] Bin Ni,[§] Ning Xie,[§] Xuhua Lu,[§] Jianlin Shi,[‡] Yi Zeng,[‡] and Xiang Guo^{*,†,§}

[‡]School of Materials Science and Engineering, University of Shanghai for Science and Technology, Shanghai, P. R. China

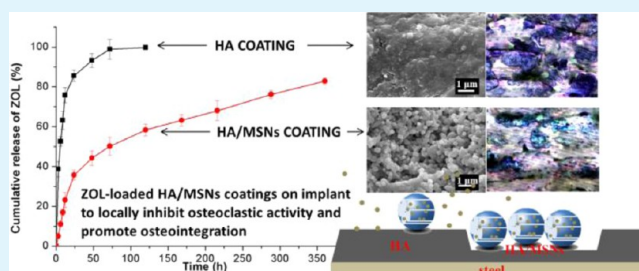
[§]Department of Orthopedics, Changzheng Hospital of the Second Military Medical University, Shanghai, P. R. China

[†]State Key Laboratory of High Performance Ceramics, Shanghai Institute of Ceramics, Chinese Academy of Sciences, Shanghai, P. R. China

S Supporting Information

ABSTRACT: In an attempt to improve implant-bone integration and accelerate bone fracture healing from resisting osteoclastic resorption point of view, we have employed a novel procedure to develop a mesoporous silica nanoparticles/hydroxyapatite (MSNs/HA) composite coating onto stainless Kirschner wire substrate. Characterizations of the surface microstructures indicated enlarged specific surface area compared to HA-coated wires as control, thus the MSNs/HA composite coated implants are endowed with abilities to locally deliver biomedical substances and enhance fracture healing. Herein, zoledronic acid (ZOL) as a model drug, different doses of which were immobilized in the mesoporous coating toward decreasing osteoclastic resorption activity. The loading capacities of ZOL increased almost eight-folds to that of pure HA coating, and the introduction of MSNs obviously retarded ZOL release to achieve a more sustained release profile. After certain periods of osteoclast like cells co-culturing with ZOL contained wires, tartrate-resistant acid phosphatases (TRAP) staining of polynucleated cells and a pit formation assay were performed to investigate the ZOL dose-dependent anti-resorption activity. The promoted local effect on osteoclasts will be of clinical benefit to support implant integration and bone repair.

KEYWORDS: mesoporous silica nanoparticles, composite coating, bisphosphonates, local release, osteoclast



1. INTRODUCTION

Research on accelerating bone fracture healing have attracted keen interests in recent years. The use of internal fixations such as interlocking intramedullary nails has marked curative effects on the treatment of long bone fraction.¹ However, for particular patients with abnormal calcium metabolism, such as postmenopausal women, bone sorption rate is obviously higher than that of bone formation which results in long term osteoporosis and hard bone fracture healing. Therefore, searching for a more effective method to promote fracture healing is becoming a research hotspot.^{2,3}

On basis of the successful application of artificial hip joint coatings, biological coated-internal fixation implants has shown great potentials in accelerating fracture healing through incorporating and locally release bioactive components.^{4,5} However, bioactive molecules like the growth factors (e.g., insulin-like growth factors, transforming growth factor- β)^{6,7} and bone morphology proteins (BMPs)⁸ have large molecular weight, thus inhibit high drug capacity. Moreover, they are prone to lose their bioactivities in the loading process, and the collection procedures cost too much. Alternatively, the third generation bisphosphonates (BPs) like nitrogen-containing zoledronic acid (ZOL) are potent inhibitors of osteoclastic bone resorption.^{9–11} Research have proved that ZOL could

regulate the balance of bone resorption through simultaneously stimulating osteoblastic secretion of osteoprotegerin (OPG) and inhibiting formation of receptor activator of nuclear factor- κ B ligand (RANKL).¹² Therefore, the incorporation of ZOL into the implant coatings to realize ZOL local administration is a valuable subject. With this method, the risks of possible systemic side effects and infections by local injection could be avoided. Furthermore, in situ release of ZOL resulted in increased bone regeneration surrounding the implants, leading to improved fixation and mechanical stability.^{13–15}

Recently, the most common coating materials on the well-established metallic implants are calcium phosphates including hydroxyapatite (HA).^{16–18} The two phosphonate groups of BPs have high affinities to the mineral phase of bone or synthetic apatite. For particularly ZOL, the amino group part forms additional N–H–O hydrogen bonds with HA.¹⁹ However, ZOL molecules chemically absorbed on the HA surface are exposed to the external fluid which might result in uncontrolled and fast drug release. Besides, biodegradable polymers have been also explored as surface modifying

Received: November 10, 2013

Accepted: March 26, 2014

Published: March 26, 2014

materials on internal fixation implants to expand their clinic use in complex bone fracture sites.^{15,20,21} Reported polymers include poly(methyl methacrylate) (PMMA),²² poly(lactic acid) (PLA),¹¹ poly(glycolic acid) (PGA),²³ or their copolymers. In this case, normally drugs like ZOL are mixed with polymer solution in advance and then obtain drug-containing polymeric surface of the implant by dip-coating step. The involving of organic solvents probably brings about toxicity or even drug inactivation issues. Moreover, previous studies have suggested that the acidic degradation products of these polymers can break the pH balance in the environment and cause further inflammation, which is not beneficial to calcification and ultimately lead to negative effects on the process of fracture healing.^{24,25}

Mesoporous materials, which have been investigated as drug delivery carriers for more than a decade,^{26–28} may provide a more advantageous alternative choice to achieve controlled and localized ZOL delivery. Chemically inert mesoporous oxides may then be of particular interest, because these can easily be combined with low molecular substances. Thereinto, mesoporous titanium oxide,²⁹ silicon oxide,^{30,31} and mesoporous bioactive glasses³² are the most studied coating materials, because of their biocompatibility, low toxicity without any pH value decreases, large specific surface area, and a pore system with tunable drug loading and release rates. It is worth noting that the coated mesoporous film preparation is based on an evaporation induced self-assembly procedure.³³ After the removal of block copolymer templates, parallel mesopores form and thus encapsulate drug molecules. However, the drug loading capacity is limited because the films are usually thin.³⁴ In the case of pure mesoporous silica coating, the bonding between the implant and bone afterwards would be weak. Moreover, without any additional covered layer, it is likely that drugs diffuse out too fast in an unsustainable pattern. Therefore, challenges of prolonged sufficient drug bioavailability and controlled drug release rate over longer period of time still exist.

In our study, on the surface of stainless Kirschner wires, a composite coating drug delivery system composed of HA and mesoporous silica nanoparticles (MSNs) is developed, which is expected to provide functions of drug delivery to resist unwanted bone resorption and accelerate fracture healing.³⁵ Different dosages of ZOL molecules were loaded respectively into pure HA coating or the composite coating. In vitro drug release tests were conducted to compare the delivery behaviors from these two surfaces. Furthermore, osteoclast like cells (OLC) were cultured with the wires with ZOL loaded or not, and a series of in vitro experiments were performed to investigate the effects of different ZOL dosages on the osteoclastic cells proliferation and resorption activity.

2. MATERIALS AND METHODS

2.1. Plasma Spraying. Commercially available stainless Kirschner wires (Shanghai Pudong Jinhuan Medical Products Co., Ltd) with a diameter of 2.0 mm and a length of 230 mm were used as the substrates in this study. HA powder with the particle size ranged from 15 to 50 μm was obtained from Sulzer Metco Co. Ltd (Switzerland). An APS system (Sulzer Metco, Switzerland) was used to fabricate HA coatings using the optimal spraying parameters listed in Table 1. The phase composition of coating is characterized by XRD, and the HA-coated sample was known as HA-w for short.

2.2. Preparation of MSNs/HA Composite Coating. HA-coated Kirschner wires were cut into pieces of 1 cm length, and were immersed in 1M HCl for 1 min, and then rinsed with deionized water.

Table 1. Plasma-Spraying Parameters

parameter	value
main gas Ar	40 slpm ^a
auxiliary gas H ₂	8 slpm ^a
arc current	550 A
arc voltage	57 V
spraying distance	300 mm
powder feeding rate	20 g min ⁻¹
gun transverse speed	250 mm/s

^a slpm = standard liter per minute.

HCl-treated wires (10 pieces) were put into ethanol (16 mL) followed by addition of 0.2 mL CTAB solution (10 wt %), 4 mL H₂O and 0.6 mL NaOH solution (0.1 M) in sequence under gently stirring. 100 μL silicon precursor tetraethoxysilane (TEOS) was firstly diluted into 2 mL by ethanol and then added dropwisely to the homogeneous mixture. The whole reaction was maintained at 37 °C for 24 h, and the wires were picked out for carefully ddH₂O rinsing and drying. Finally, as-synthesized coated wires were calcined at a rate of 2 °C/min for 4 h to remove the templates. The MSNs/HA composite wires were named as H/M-w.

2.3. Characterizations. The whole coating process was characterized by scanning electron microscopy (SEM, FEI Quanta 450) through observations of the wire surface morphology at certain stage of reaction, and the compositions of different coatings were also examined using energy diffraction spectroscopy (EDS). The MSN/HA composite powders were carefully scraped from the coated wires and then observed with transmission electron microscopy (TEM, JEOL 2010).

2.4. ZOL Loading and in Vitro Release Test. Zoledronic acid was resolved in ultrapure water to form solutions with drug concentrations of 5 $\mu\text{g/mL}$, 10 $\mu\text{g/mL}$ and 20 $\mu\text{g/mL}$ respectively. To load ZOL into the external coatings of HA-w and H/M-w wires, 4 pieces of each (1 cm in length) were soaked in 10 ml of these three ZOL solutions for 3 days. The remained solutions after soaking were kept for further examinations.

In vitro release of ZOL from drug-loaded HA-w and H/M-w wires were carried out in 3 mL of 0.01 M phosphate buffered saline (PBS) at 37 °C. One hundred microliters of the release medium was withdrawn at pre-determined time intervals and replaced by fresh prewarmed PBS every time.

The ZOL concentrations of all solutions were determined using a reverse phase high-performance liquid chromatography (HPLC, Agilent 1260) technique with C18 column (200 mm \times 4.6 mm, 5 μm), 1 mL/min flow rate and ultraviolet detection at 215 nm. The mobile phase was composed of 25 vol % acetonitrile and 75 vol % buffer solution (8 mmol/L Na₂P₂O₇, 20 mmol/L tetrabutylammonium hydroxide, TBHA) whose pH value was adjusted at 6.8 by adding phosphoric acid.

2.5. In Vitro Cytotoxicity Evaluation. In vitro cytotoxicities of commercial Kirschner wires, HA-w and H/M-w wires were evaluated using MTT assay. L-929 cells were seeded in 24-well cultured plates at a density of 5×10^3 per well with 1 mL culture medium (DMEM; 10% fetal calf serum). After 24 h of adhesion, one piece of each wire (1 cm length) sample was added with the help of cell culture inserts (0.4 μm , Nunc GmbH & Co. KG, Germany) to avoid cell-material contacts, and the tissue culture plates without samples were used as control. On specific days, the medium and materials were removed, then 1 mL of 0.5 mg/mL MTT solution was added and cells were incubated for another 4 h. Upon removal of the MTT solution, the purple formazan crystals were dissolved in 1 mL of dimethyl sulfoxide (DMSO) by shaking the plate for 10 min. The solutions were then centrifugalized and the supernatants were transferred into another plate to record absorbance at 490 nm on a micro-plate reader (Bio-Tek ELx800).

2.6. In Vitro Osteoclast Like Cell Culture. Mice preosteoclasts and osteoclasts were generated as described.³⁶ Briefly, isolated bone marrow-derived monocytes (BMMs, 3×10^6 /well) from mice were seeded in 24-well plates to allow cell-to-cell contact and cultured in a

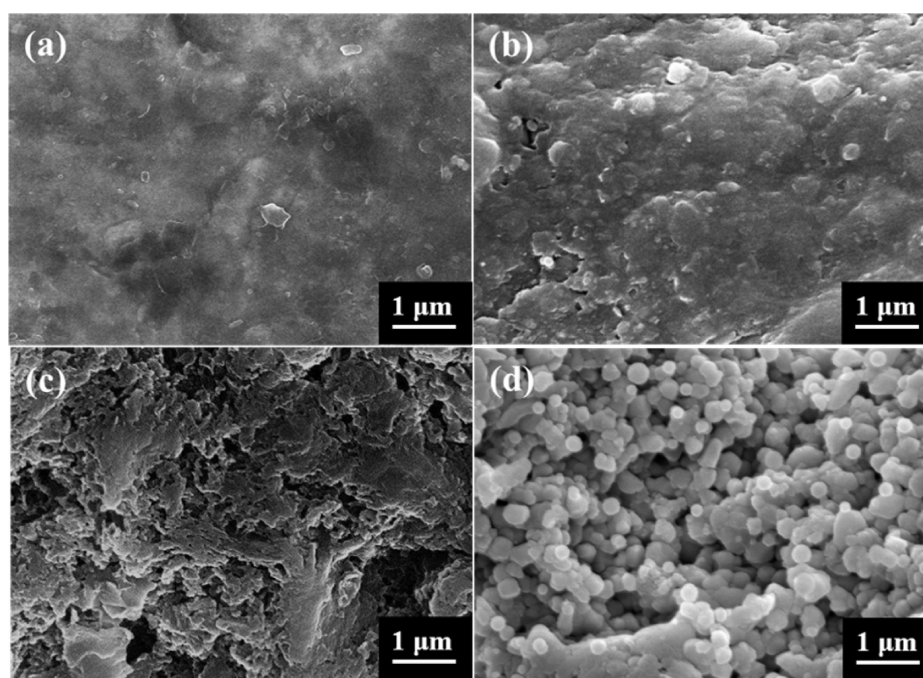


Figure 1. SEM images of the different wire surfaces after certain treatment during the H/M-w preparation (a) original Kirschner wire, (b) HA-w wire, (c) HCl-treated HA-w wire, (d) H/M-w wire.

MEM containing 10% FBS added 50 ng/mL recombinant M-CSF for 3 days to generate preosteoclasts. After 3 days, 20 ng/mL recombinant macrophage colony stimulating factor (M-CSF), 40 ng/mL recombinant nuclear factor- κ B ligand (RANKL) and wires were added to generate mature osteoclasts. Tissue Culture Inserts shown in Figure 6s in the Supporting Information, 0.4 μ m (Nunc GmbH & Co. KG, Germany) were used to allow addition of the wires to the cell culture in a noncontact manner. During the time of incubation with drug-loaded wires, the medium was not changed but controlled regularly and refilled in case of evaporation. As controls, cells were also cultured without any wire materials or with non-ZOL-loaded wires (pure Kirschner wire, HA-w, and H/M-w) following the same procedure above. All the results were recorded at 7, 9, and 11 days, respectively.

2.7. Determination of Osteoclasts/TRAP Assay. Tartrate-resistant acid phosphatases (TRAP) staining was used as a marker for mature osteoclasts. After cultivation of the cells with ZOL-loaded wires for specific periods, the cells were fixed for 5 min with 3.7% buffered formaldehyde and stained for TRAP by adding naphtol AS-MX phosphate and fast red violet. Polynucleated TRAP-positive cells were counted using a microscope (Carl Zeiss Microscope, Germany) equipped with a camera and an image analysis system to mark and count the cells. Results were analyzed in relation to total cell number of the control groups, which were coated wire samples without ZOL loaded. Settings were performed in triplicate measurements and repeated twice ($n = 6$).

2.7. Osteoclast Activity/Pit Formation Assay. Bone resorption activity was assessed by pit formation assay according to previous reports with slight modification.³⁷ BMMs were cultured on bovine cortical bone slices in 24-well plates and induced by MCSF for 3 days. Then additional 20 ng/mL of recombinant M-CSF and 40 ng/mL of recombinant RANKL were added to the medium. After application of ZOL-loaded coated wires the cells were cultured for further 4–8 days. At predetermined time interval the slices were placed for 10 min in 1 M NH_4OH and were sonicated to remove the cells. The cell-free slices were stained in 1% toluidine blue in 1% sodium borate for 3 min. The resorption pits appeared dark blue and were viewed by light microscopy. The percentage of pit area to a “random field of view” was counted. Results were analyzed in relation to total pit area of the non-ZOL loaded control group. Settings were performed in triplicate measurements and repeated twice ($n = 6$).

Statistical analysis: Statistics were performed using ANOVA for independent samples. All data were expressed as mean \pm standard deviation. Statistical differences were defined at a 95% confidence level. Statistical comparison of data was supported by SPSS (release 10.0; SPSS Chicago, IL).

3. RESULTS

3.1. Morphology and Microstructure Characterizations. The XRD patterns of original HA powders and HA powders scraped from coatings on HA-w or H/M-w wires are shown in Figure 2s in the Supporting Information, which is seen that the main HA diffraction peaks maintained and some new phases of CaO and tricalcium phosphate appeared due to the decomposition during high-temperature plasma spaying. The process to coat HA/MSN composites onto Kirschner wires was evidenced by SEM observations. The surface morphology of untreated commercial wires, HA plasma-sprayed and acid pretreated afterward wires, and MSN/HA-coated samples are shown in Figure 1. It suggests that the smooth surface evolved to a comparative rough one after plasma-spraying of HA. The HA coating composed by melted flat particles seemed fairly dense. However, a short period of diluted acid corrosion produced plenty of defects and holes which might be beneficial for the followed chemical growth of MSNs. As expected, Figure 1d indicates that the holes were filled with large amounts of newly formed spherical particles, and most of the nanoparticles strongly bound to the established HA coating or in between each other. From additional SEM images with lower magnification of the cross-section of the coatings shown in Figure 3s in the Supporting Information, MSNs particles did not only grow in the holes but also gradually covered all the HA coatings. The thicknesses of HA and MSNs layers were approximate 30 μ m and 1 μ m, respectively. After mesoporous phase deposition, the wire's surface became more nano-structured.

To obtain more microstructure information, the final composite coating was scraped out from the wires and

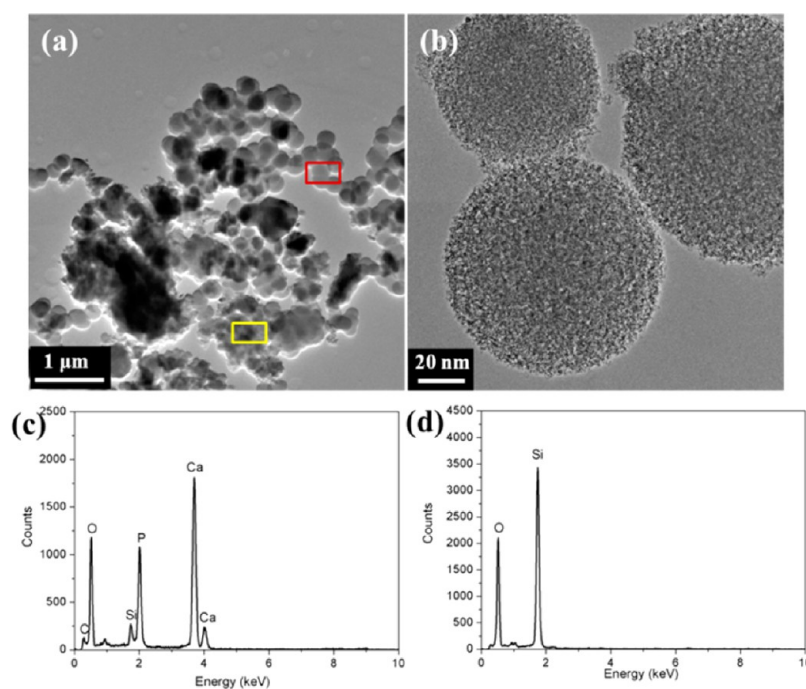


Figure 2. TEM images of (a) the scraped powders from H/M-wires; (b) MSNs in the composite coating and EDS spectra of corresponding framed areas in a: (c) yellow square; (d) red square.

investigated using TEM and N_2 sorption characterizations. This coated powder was obviously a composite of irregular crystallized HA particles and some silica nanospheres according to Fig. 2. Moreover, the EDS results of the composite displayed typical Ca, P, Si, and O peaks indicating HA/silica composition. The magnified TEM image of the nanospheres in Figure 2b shows mesoporous structures without ordering and correspondingly the EDS spectrum shows the pure Si–O composition of the nanospheres. Furthermore, FI-IR spectra illustrated consistent results as shown in Figure 4s in the Supporting Information.

Figure 3 reports the nitrogen adsorption/desorption isotherms for both scraped HA powders and HA/MSNs composite powders. Isotherms of the composite exhibited a small pore filling jump at P/P_0 around 0.2 and its BJH pore diameter calculated from the desorption branch is about 2.5 nm, which is another convincing evidence for the mesoporous

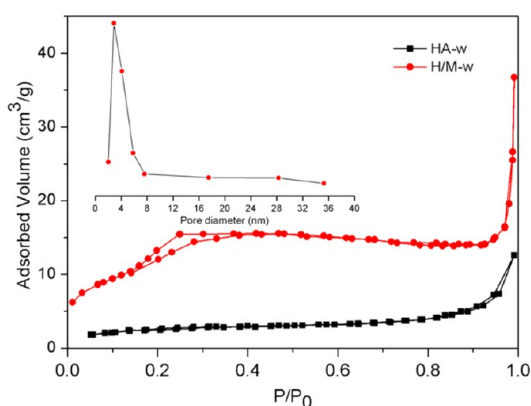


Figure 3. N_2 sorption isotherms and pore size distribution (inset) of the powder scraped from H/M-wires (red), and isotherms of coated powders from HA-w wires.

nature of the nanospheres. Comparatively, no pore filling associated with mesopores is observed of pure HA coatings. The BET specific surface area of the composites was calculated to be $97 \text{ m}^2/\text{g}$, i.e., some 10 times higher than that of HA powders because of the nonporous structure.

3.2. Drug Loading and Release. Previous research³⁸ has reported the success encapsulation of biphosphonate drugs, zoledronate as one of them as well, into mesoporous bioceramics, and represented sustained release properties. Here in our study, the MSNs in the composite coating also undertake the main responsibility to load ZOL molecules. As expected, in Figure 4a is shown that the ZOL drug loading amounts of H/M-w were much higher than that of HA-w. The HA coating alone is speculated to trap ZOL molecules through chemical associations according to previous studies about BP-containing apatites,¹⁹ hence the limited surface area of HA-w restricted large amounts of ZOL to bind. However, the mesopores greatly enlarged the surface area and then host more ZOL drugs into the coating. In addition, the ZOL loading capacities are initial drug concentration-dependent for both HA-w and H/M-w, namely increased ZOL concentrations leading to higher capacities. For instance, H/M-w wires loaded around $14.06 \mu\text{g}/\text{cm}$ ZOL after soaking in $20 \mu\text{g}/\text{mL}$ ZOL solution, whereas the value was as low as $4.48 \mu\text{g}/\text{cm}$ for the wires immersed in $5 \mu\text{g}/\text{mL}$ original drug solution. The reason is that a higher concentration difference gives rise to a larger driving force for drugs to enter the nanopores.³⁹

The release profiles of ZOL from HA-coated wires as references and HA/MSNs composite-coated wires are shown in Figure 4b. In agreement with the former literature,¹³ ZOL drugs were almost completely released from the surface of HA-coated wires in the first 3 days. In contrast, for all the ZOL-loaded H/M-w wires, on which both MSNs and HA were coated, presented more sustained drug release patterns. Taking H/M-w-10 for an example, a severe initial burst release of ZOL is observed during the first day, which accounts for around 50%

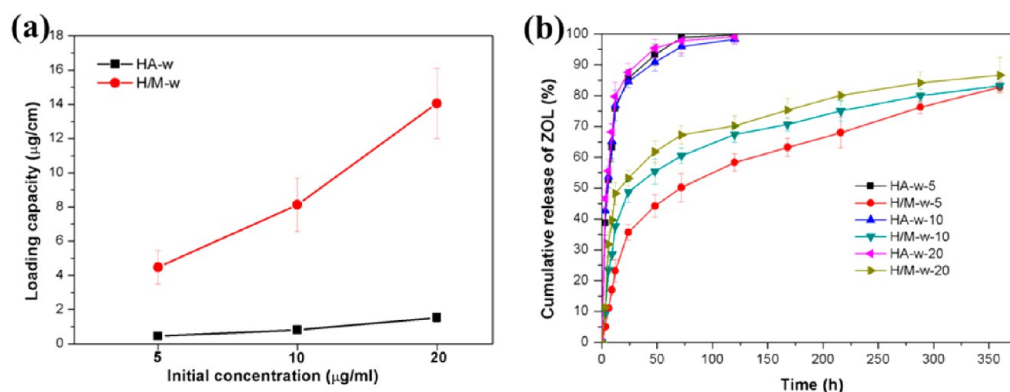


Figure 4. (a) ZOL drug loading amounts and (b) in vitro release curves in PBS at 37 °C from HA-w wires and H/M-w wires loaded with different doses of ZOL, respectively.

of the total loaded from the coatings. The reason for the burst release can be probably attributed to the loss of drugs attached on the HA coating and the outer surface of mesoporous particles as well. It is noticed that such a burst release percentage is significantly smaller than that from pure HA-coated samples as illustrated in Figure 4b, which already suggests an important role that mesopores played for maintaining drug molecules. Subsequently, another 30% dose of ZOL was released in a comparatively sustained manner and lasted for more than 10 days. For comparison, it can be found that drugs released slightly faster in the early stage if more drugs were encapsulated, while the total release percentages tended to be close with time going on. This means that the percentage of drugs trapped in the mesopores is lower when higher initial ZOL concentration is used, and the nanoscale pores are not only able to load much higher dosage of ZOL drugs but also preserve ZOL molecules for a longer release period, which is thus considered to be favorable to inhibit bone resorption and promote new bone formation.

3.3. Cytotoxicity. Cell toxicity of the wire materials was analyzed using MTT assay after 1, 3, and 7 days of culture. As shown in Figure 5, an increase in absorbance from day 1 to day 7 was recorded, which indicates that the cells were viable with the wires or coated wires around. Moreover, the proliferation behavior of cells with different wires was very similar to each other on every measurement day. Having been clinically used

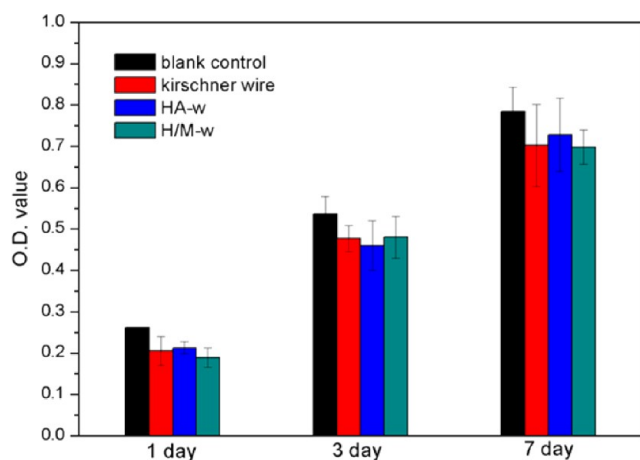


Figure 5. Viabilities of L-929 fibroblasts cultivated with bare Kirschner wires, HA-w wires, and H/A-w wires.

for bone tissue engineering, the low cell toxicity and excellent biocompatibility of HA apatites were already widely accepted. Therefore, the results shown in Figure 5 approved that the introduction of MSNs onto the HA-coated Kirschner wires would add no additional cell toxicity to them.

3.4. Trap Staining Assay. In vitro tests to evaluate the use of zoledronic acid towards osteoblasts and osteoclasts, such as the total cell number, relative protein synthesis (OPG, sRANKL etc.) and new bone generation ability, were repeatedly carried out. Osteoclasts are one major target of bisphosphonates in order to inhibit bone resorption. This effect is therapeutically used in pathologies with elevated osteoclastic activity. The aim of this study was to further investigate the local application of ZOL in different dosages to osteoclasts for different culture durations, with a special focus on osteoclast number and resorption activity.

Trap-positive multinucleated cells could be clearly identified after setting as shown in Figure 5s in the Supporting Information, which illustrates the success of osteoclast-induced formation.

The results obtained on osteoclast culturing with ZOL loaded HA-w and H/M-w wires for 7, 9, and 11 days respectively are reported in Figure 6a, and the number of TRAP positive cells was normalized to the total osteoclast number of non-ZOL wires control. Because the drug release was a continuous procedure and no medium was discarded during the cell culture, osteoclast formation which was directly decided by ZOL concentration could thus reveal the amounts of ZOL in the culture medium. At each specific day, it is found that the numbers of osteoclasts co-cultured with H/M-w wires were significantly fewer compared to that with HA-w wires. For example, at day 7, nearly 90% to the total control of mature osteoclasts were observed when cultured with HA-w-SZOL and the value was 54% of H/M-w-SZOL. The differences could be explained using the in vitro drug loading and release results (Figure 4). Significant higher ZOL capacity in H/M-w wires, because of the presence of mesoporous phase, causes more osteoclast apoptosis. This dosage dependent effect was also evidenced among the samples with different ZOL loaded amounts within the same group. There is a significant decrease after exposure to wires which are loaded with higher ZOL dose. Moreover, the cell number decrease trend along with the culture time was not very sharp, which coincided with the drug release profile. In the later stage, much less ZOL drugs were newly freed from the coatings.

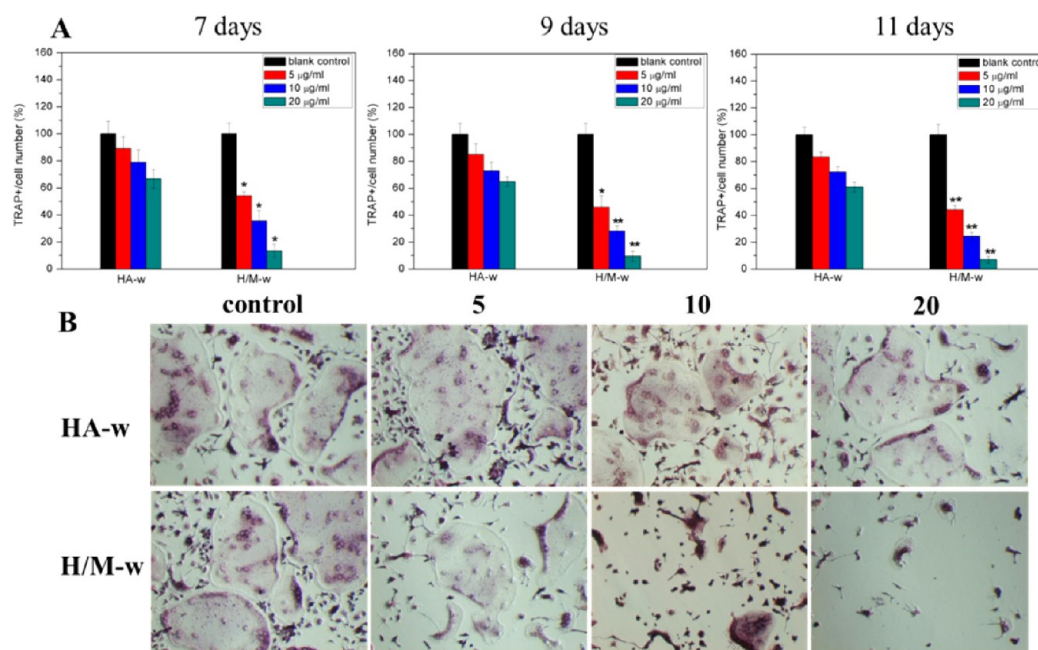


Figure 6. (A) TRAP-positive cell numbers at 7, 9, 11 days; (B) optical images of TRAP-staining cells under 11 days culture with exposure to the two groups of coated ZOL-loaded wires; * $p \leq 0.05$ if compared with both HA-w and blank control, ** $p \leq 0.005$ if compared with both HA-w and blank control. The blank control refers to non-ZOL-loaded HA coated wires or H/M composite coated wires, respectively.

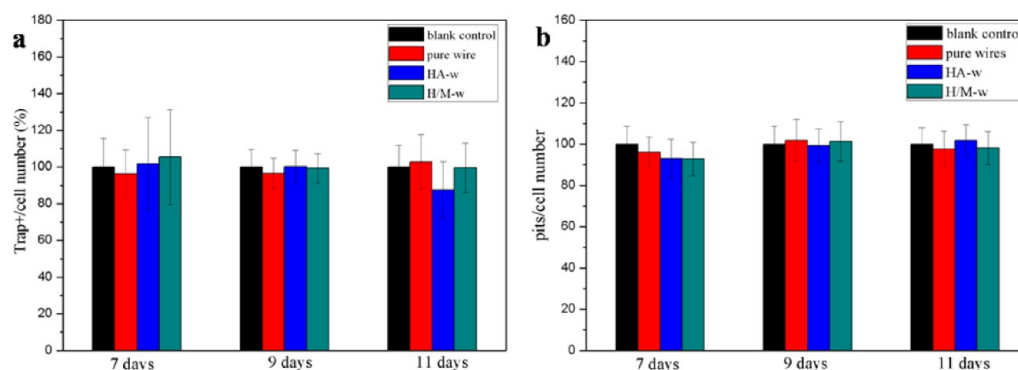


Figure 7. Under 7, 9, and 11 days culture with exposure to different wire specimen: pure stainless wire, HA-w wire, and H/M-w wire respectively, (a) normalized TRAP-positive cell numbers to control; (b) normalized pit areas to control. The blank control refers to result out of cell cultures without any sample wires adding in.

Optical images of TRAP-stained cells after 11 days culturing listed in Figure 6b further confirmed the statistic data and results. It shows that exposure to wires with higher ZOL concentration brings about an obvious decline in osteoclast numbers.

Without any ZOL drug loaded, the potential influences of wire materials including pure stainless wire, HA-w and H/M-w to osteoclasts were examined by involving in cell cultures. The results in Figure 7a showed that no significant difference of TRAP positive number was detected among all tested groups. It reveals that HA and MSNs materials under this noncontact manner barely exert marked impacts to the formation of osteoclasts out of precursor cells, and thereafter osteoclasts' viability and proliferation as well.

When pure ZOL substances of the quantities as loaded in H/M-w coatings were directly applied to the culture medium, i.e., 4.5, 8.0, and 14 $\mu\text{g}/\text{mL}$, TRAP positive cells showed a more remarkably decrease after 7 days compared to the corresponding H/M-w sample. For instance, according to the statistics data and microscope pictures in Fig.8, less than 40% mature

osteoclasts were observed and after exposure to 14 $\mu\text{g}/\text{mL}$ of ZOL, almost 98% osteoclasts disappeared. However, the TRAP positive cell number became higher again at day 9 and day 11 probably due to ZOL consumption and thereby ZOL concentration declined.

3.5. Pit Formation Assay. The pit formation assay was used to evaluate the influence of ZOL coated implants on the resorption activity of osteoclasts. The assay enables to mimic the activity of osteoclasts in vivo. Results showed a significant dose-dependent decrease in global osteoclast resorption activity estimated as a decrease in number of resorption areas (pits) on bone chips. This effect was shown after exposition to HA-w and H/M-w again for 7, 9, and 11 days. As depicted in Figure 9a, the decrease in pits was extraordinary significant ($p < 0.01$) for HA-w wires at initial concentrations of 20 $\mu\text{g}/\text{mL}$ and all the H/M-w wires. At day 11, in comparison to HA-w wires, it is showed in Figure 9b that H/M-w wires with mesoporous structure could inhibit osteoclastic resorption activity and the formation of bone resorption more efficiently, and the depressing effect could sustain longer time.

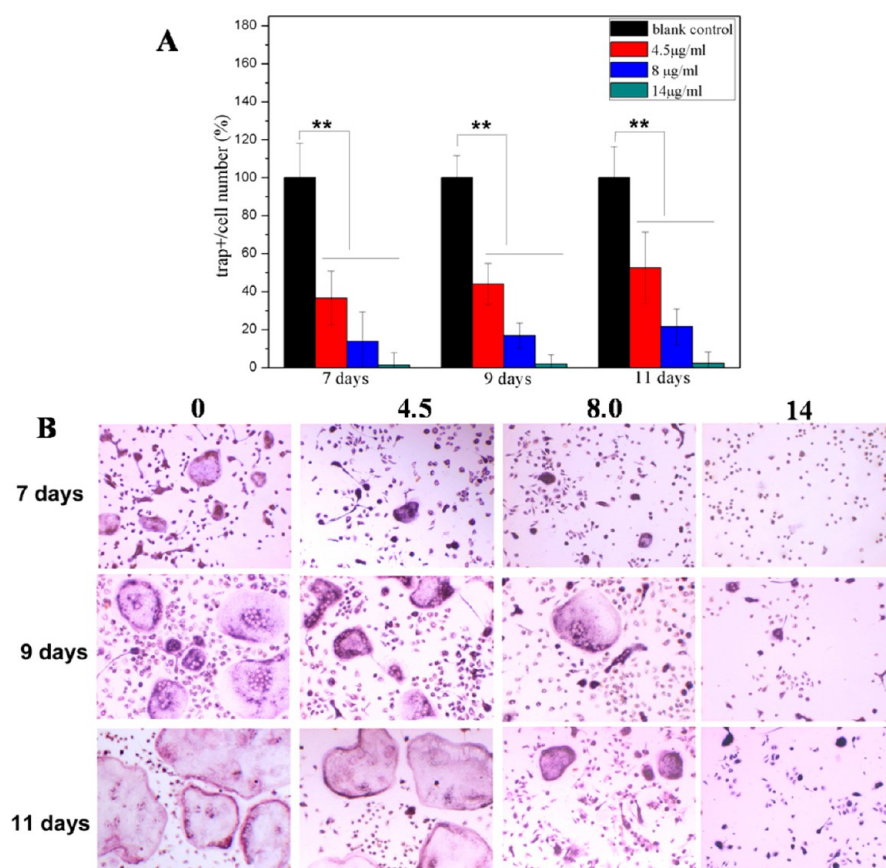


Figure 8. Under 7, 9, and 11 days culture with exposure to pure ZOL substances with different concentrations: 4.5, 8.0, and 14 $\mu\text{g}/\text{mL}$, respectively; (A) normalized TRAP-positive cell numbers to control; (B) optical images of TRAP-positive cells. The blank control refers to result out of cultures without additions of ZOL drugs.

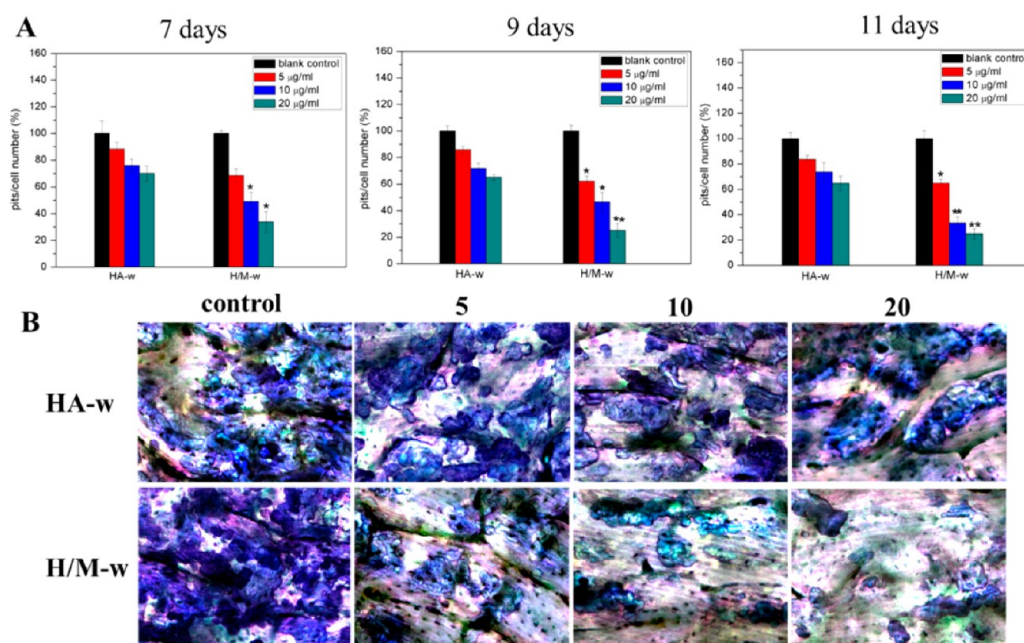


Figure 9. (A) Pits area normalized to control with mature osteoclast culture for 7, 9, 11 days; (B) Optical images of stained resorption lacuna under 11 days culture with exposure to the two groups of coated ZOL-loaded wires; * $p \leq 0.05$ if compared with both HA-w and blank control, ** $p \leq 0.005$ if compared with both HA-w and blank control. The blank control refers to non-ZOL-loaded HA coated wires or H/M composite coated wires, respectively.

Similarly to the TRAP counting results, Figure 7b shows that either pure Kischner wires or wires coated with HA or H/M

composite entirely had no noticeable influence on the osteoclastic bone resorption activity. In like manner as well,

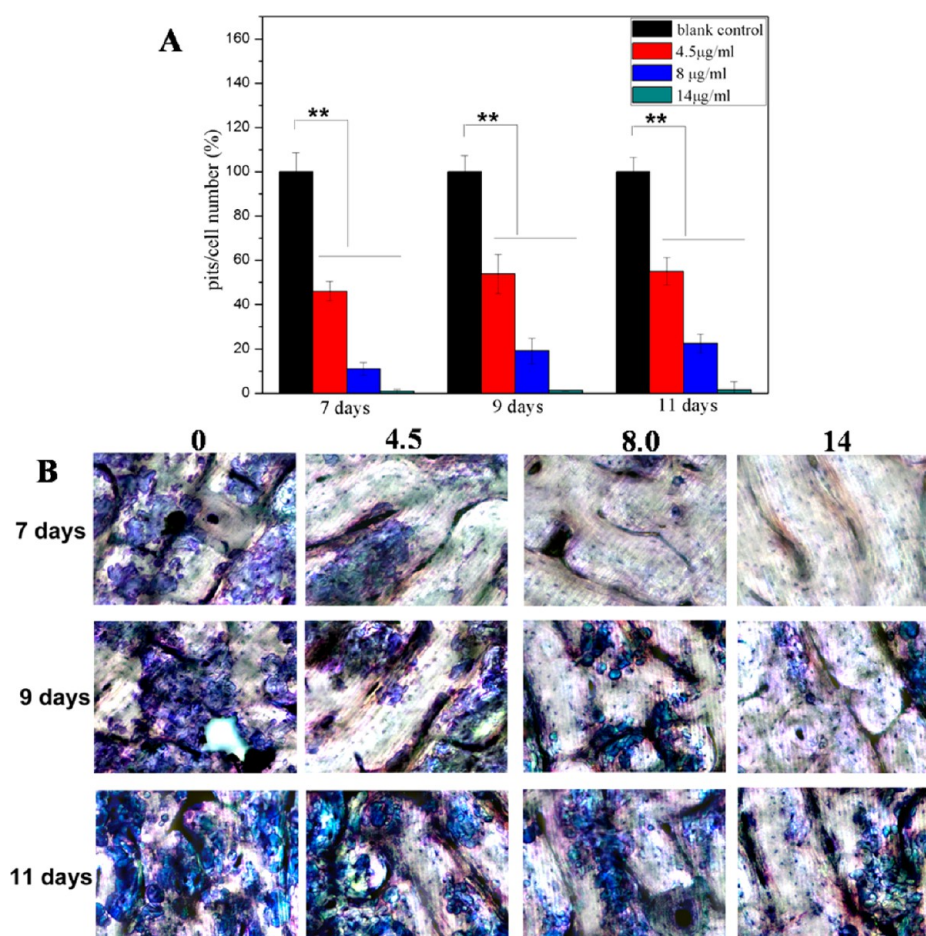


Figure 10. Under 7, 9, and 11 days culture with exposure to pure ZOL substances with different concentrations: 4.5, 8.0, and 14 $\mu\text{g}/\text{mL}$ respectively, (A) normalized pits area to control; (B) optical images of stained resorption lacuna. Blank control refers to result out of cultures without additions of ZOL drugs.

results in Figure 10 indicates that comparable amounts of ZOL pure substances application towards osteoclasts led to sharply decreased pits areas.

4. DISCUSSION

HA coating on implants, which mimic the main inorganic component of extracellular bone matrix, has been confirmed in either experimental or clinical settings that it can support the growth of osteoprogenitor cells from the host into the external coating structure of the implant. However, studies suggested that single bone conduction from HA coatings was not sufficient in bone fracture healings, particularly at the early stage. On one hand, for a special population like postmenopausal women or elders with turnover balances of bone metabolism, i.e., osteoclastic activity is more significant than osteogenic activity, HA-coated wires are not enough to favor the formation of original callus and the bridge of fracture fragments as well. On the other hand, people found that HA particles are susceptible to periprosthetic bone resorption⁴⁰ and subsequent implant failure, which is why bisphosphonates are prescribed at this time point.⁴¹ The approach to load bisphosphonates during implantation would overcome the disadvantages of oral or systemic administrations. Strategies of developing BP-modified calcium phosphates including HA were widely investigated for local administration of BPs. However, directly synthesis of crystallized BP-modified HA is an uneasy

task with the presence of BPs because of its high affinity to HA. Therefore, most of the attempts to prepare the composites have been performed through chemisorption from solution, though the BP loading capacity is limited.⁴² To achieve sufficient drug loading capacity, more sustained release rate over longer periods of time, and lower clinical costs, mesoporous silica-based matrices were very useful in this context, because of their low toxicity, biostability, and large specific surface area.

Herein, mesoporous silica nanoparticles were in-situ fabricated in plasma-coated HA on the surface of metallic internal fixation wires. The characterization results have clearly indicated that the in situ growth method was effective to achieve mesoporous silica nanoparticles onto the external coating. In the procedures for synthesizing MSNs, the former HA coating, which usually carry negative charges in distilled water as shown in Table 1s in the Supporting Information, could assist the adsorption of positively charged surfactant micelles with suitable concentration. Subsequently silicon precursor precipitated onto the adsorbed micelles and self-assembled to form mesostructured inorganic/organic composite nanospheres under an alkaline condition. Upon calcination, the surfactants were removed leading to formation of mesoporous silica. Therefore, the amounts of MSNs could be controlled by adjusting the reaction parameters. More importantly, the whole reaction did no harm to the original HA coating, thus the HA/MSNs-coated wires are still able to bond to natural bone tissues. In addition, the pull-out tests

showed no decline of the bonding strength between the coating and the substrate after MSNs developing (Figure 7s in the Supporting Information).

Compared to reported homogeneous mesoporous oxide coatings, MSNs exhibited superiorities in terms of the two essential parameters of drug eluting implants: drug loading capacity and drug release manner. The amounts of cargoes in the surface coating were determined by the surface area and pore volume. In this case, when MSNs with disordered mesopore structure were set in HA coating, ~ 10 times larger surface area was observed. Consequently, zolendronic acid as the model drug uptake by the MSNs-containing composite coating increased to ~ 8 times higher compared with pure HA coating, which is slightly less than the increased value of surface area. If one then assumes a diffuse distance of 1 mm in vivo, the distribution volume is on the order of 0.1 cm^3 and the resulting ZOL concentration then is on the order of $\sim 10 \text{ }\mu\text{g/mL}$. This value apparently fulfills the clinical requirements. For certain conditions, the ultimate release amounts of ZOL could be also adjusted through changing the loading ZOL concentration.

The second key parameter is the drug release rate. For mesoporous drug carriers, it was shown previously that this is controlled mainly by diffusion out from the mesoporous structure, namely, pore size.⁴³ Reported mesoporous oxide films on the surface of implants were usually prepared using block copolymers through solvent evaporation procedure, thus obtained larger mesopore diameters (normally $>4 \text{ nm}$) compared with the pores ($\sim 2.5 \text{ nm}$) formed under the direction of smaller CTAB molecules, as well as parallel mesopore channels. Therefore, the more restricted drug container and more three dimensional pore distributions within the nanospheres have supplied more resistance to the drug transportation. On the other hand, additional layers outside the mesoporous oxide films, for example di-octyltetramethyl disilazane, were often applied to delay the drug release. However, herein a large part of MSN particles were embedded in the HA coating holes, and furthermore they pile up to detain the ZOL diffusion out. In addition, regardless of the initial ZOL concentrations, there were still a small part of the whole loaded ZOL sustainedly release after 1 week, which could maintain a particular drug level in the bone cavity. As controls, comparable amounts of pure ZOL substances resulted in much higher toxicities towards mature osteoclast proliferation and its bone resorption activity in the first week. However, this inhibition effect did not last any more later on because of the consumption of ZOL. Gradually lower ZOL concentrations and increased osteoclast numbers would harm new bone generation.

Overall, a sustained release of ZOL from MSNs/HA composite coating leads to the "higher concentration in the early stage and lower in the later" pattern of ZOL, which is beneficial on osseous implant integration. According to Greiner SH et al.,¹⁵ high concentration of ZOL in the early stage could delay the remodeling of callus and thus avoid precocious removal of primary callus before the fracture fragments are bridged, so that the cumulative primary callus stabilizes the implant. After decrease of release rate and drug diminution, remodeling recovers to normal and early callus is transformed into mature callus, which leads to successful osseous regeneration. However, in the case of ZOL directly absorbed on the HA apatite, the release medium was easily able to dissolve ZOL on the exposed surface, thereby speeding up release kinetics.

5. CONCLUSIONS

The stainless Kirschner wires were successfully coated with in situ fabricated mesoporous silica nanoparticles and plasma-sprayed hydroxyapatite. Much larger amounts of ZOL drug were encapsulated into the mesoporous composite coatings compared to pure HA coatings, and the loading capacity could be adjusted in a wider range because of the large specific surface area of MSNs. The composite-coated wires also showed more sustained drug release rates and could provide sufficient drug concentrations over longer time. The exposure of these ZOL composite-coated wires to osteoclastic cells leads to obvious hampers of osteoclast proliferation and bone resorptive activity, and therefore the MSN/HA-coated wires may show potential in promoting fracture healing.

Further in vivo studies are presently being carried out in our group to evaluate the formation of original callus and the bridge of fracture fragments with aids of pure or coated or ZOL-containing coated wires. Preliminary outcomes have already confirmed in vitro results, and more investigations on their effects of bone fracture healing are still to be executed further on.

■ ASSOCIATED CONTENT

📄 Supporting Information

Additional characterizations of the coatings including XRD, FT-IR spectra, more SEM images, surface ζ -potential and adhesion strength were shown. A HPLC analyze method and noncontact pattern of cell culture were explained. This material is available free of charge via the Internet at <http://pubs.acs.org/>.

■ AUTHOR INFORMATION

Corresponding Author

*E-mail: gx9601074@gmail.com. Tel: 086-021-81886829.

Author Contributions

†M.Z. and X.G. contributed equally to this manuscript.

Notes

The authors declare no competing financial interest.

■ ACKNOWLEDGMENTS

This work was supported by the National Nature Science Foundation of China (Grants 81101343 and 51302170) and Science Foundation of Health Bureau, Shanghai Municipal Government, P. R. China (Grant 2011254).

■ REFERENCES

- (1) Kempf, I.; Grosse, A.; Beck, G. Closed Locked Intramedullary Nailing. Its Application to Comminuted Fractures of the Femur. *J. Bone Jt. Surg., Am. Vol.* **1985**, *5*, 709–720.
- (2) Jakob, F.; Seefried, L.; Ebert, R.; Eulert, J.; Wolf, E.; Schieker, M.; Bocker, W.; Mutschler, W.; Amling, M.; Pogoda, P.; Schinke, T.; Liedert, A.; Blakytyn, R.; Ignatius, A.; Claes, L. Fracture Healing in Osteoporosis. *Osteologie* **2007**, *2*, 71–84.
- (3) Grote, S.; Boecker, W.; Mutschler, W.; Schieker, M. Current Aspects of Fragility Fracture Repair. *Eur. J. Trauma Emerg. Surg.* **2008**, *6*, 535–541.
- (4) Paglia, D. N.; Wey, A.; Breitbart, E. A.; Faiwizewski, J.; Mehta, S. K.; Al-Zube, L.; Vaidya, S.; Cottrell, J. A.; Graves, D.; Benevenia, J.; O'Connor, J. P.; Lin, S. S. Effects of Local Insulin Delivery on Subperiosteal Angiogenesis and Mineralized Tissue Formation During Fracture Healing. *J. Orthop. Res.* **2013**, *5*, 783–791.
- (5) Wu, K. M.; Song, W.; Zhao, L. Z.; Liu, M. Y.; Yan, J.; Andersen, M. O.; Kjems, J.; Gao, S.; Zhang, Y. M. MicroRNA Functionalized Microporous Titanium Oxide Surface by Lyophilization with

Enhanced Osteogenic Activity. *ACS Appl. Mater. Interfaces* **2013**, *7*, 2733–2744.

(6) Wildemann, B.; Kadow-Romacker, A.; Lubberstedt, M.; Raschke, M.; Haas, N. P.; Schmidmaier, G. Differences in the Fusion and Resorption Activity of Human Osteoclasts after Stimulation with Different Growth Factors Released from a Polylactide Carrier. *Calcif. Tissue Int.* **2005**, *1*, 50–55.

(7) Wildemann, B.; Lubberstedt, M.; Haas, N. P.; Raschke, M.; Schmidmaier, G. IGF-I and TGF-beta 1 Incorporated in a Poly(D,L-lactide) Implant Coating Maintain Their Activity over Long-term Storage - Cell Culture Studies on Primary Human Osteoblast-like Cells. *Biomaterials* **2004**, *17*, 3639–3644.

(8) Baltzer, A. W. A.; Lattermann, C.; Whalen, J. D.; Wooley, P.; Weiss, K.; Grimm, M.; Ghivizzani, S. C.; Robbins, P. D.; Evans, C. H. Genetic Enhancement of Fracture Repair: Healing of An Experimental Segmental Defect by Adenoviral Transfer of the BMP-2 Gene. *Gene Ther.* **2000**, *7*, 734–739.

(9) Reinholz, G. G.; Getz, B.; Pederson, L.; Sanders, E. S.; Subramaniam, M.; Ingle, J. N.; Spelsberg, T. C. Bisphosphonates Directly Regulate Cell Proliferation, Differentiation, and Gene Expression in Human Osteoblasts. *Cancer Res.* **2000**, *60*, 6001–6007.

(10) Teitelbaum, S. L. Bone Resorption by Osteoclasts. *Science* **2000**, *289*, 1504–1508.

(11) Rogers, M. J.; Crockett, J. C.; Coxon, F. P.; Monkkinen, J. Biochemical and Molecular Mechanisms of Action of Bisphosphonates. *Bone* **2011**, *49*, 34–41.

(12) Hofbauer, L. C.; Gori, F.; Riggs, B. L.; Lacey, D. L.; Dunstan, C. R.; Spelsberg, T. C.; Khosla, S. Stimulation of Osteoprotegerin Ligand and Inhibition of Osteoprotegerin Production by Glucocorticoids in Human Osteoblastic Lineage Cells: Potential Paracrine Mechanisms of Glucocorticoid-Induced Osteoporosis. *Endocrinology* **1999**, *140*, 4382–4389.

(13) Gao, Y.; Zou, S. J.; Liu, X. G.; Bao, C. Y.; Hu, J. The Effect of Surface Immobilized Bisphosphonates on the Fixation of Hydroxyapatite-Coated Titanium Implants in Ovariectomized rats. *Biomaterials* **2009**, *30*, 1790–1796.

(14) Wermelin, K.; Suska, F.; Tengvall, P.; Thomsen, P.; Aspenberg, P. Stainless Steel Screws Coated with Bisphosphonates Gave Stronger Fixation and More Surrounding Bone Histomorphometry in Rats. *Bone* **2008**, *42*, 41.

(15) Greiner, S.; Kadow-Romacker, A.; Wildermann, B.; Schwabe, P.; Schmidmaier, G. Bisphosphonates Incorporated in a Poly(D,L-lactide) Implant Coating Inhibit Osteoclast Like Cells *In Vitro*. *J. Biomed. Mater. Res., Part A* **2007**, *83*, 1184–1191.

(16) Niu, S.; Cao, X. R.; Zhang, Y.; Zhu, Q. S.; Zhu, J. Y.; Zhen, P. Peri-implant and Systemic Effects of High-/Low-Affinity Bisphosphonate-Hydroxyapatite Composite Coatings in a Rabbit Model with Peri-implant High Bone Turnover. *BMC Musculoskeletal Disord.* **2012**, *13*, 97.

(17) Liu, D. M.; Yang, Q. Z.; Troczynski, T. Sol-gel Hydroxyapatite Coatings on Stainless Steel Substrates. *Biomaterials* **2002**, *23*, 691–698.

(18) Choudhury, P.; Agrawal, D. C. Sol-gel Derived Hydroxyapatite Coatings on Titanium Substrates. *Surf. Coat. Technol.* **2011**, *206*, 360–365.

(19) Boanini, E.; Torricelli, P.; Gazzano, M.; Fini, M.; Bigi, A. The Effect of Zoledronate-Hydroxyapatite Nanocomposites on Osteoclasts and Osteoblast-like Cells *In Vitro*. *Biomaterials* **2012**, *33*, 722–730.

(20) Greiner, S.; Kadow-Romacker, A.; Schmidmaier, G.; Wildemann, B. Cocultures of Osteoblasts and Osteoclasts are Influenced by Local Application of Zoledronic Acid Incorporated in a Poly(D,L-lactide) Implant Coating. *J. Biomed. Mater. Res., Part A* **2009**, *91*, 288–295.

(21) Greiner, S.; Kadow-Romacker, A.; Lubberstedt, M.; Schmidmaier, G.; Wildemann, B. The Effect of Zoledronic Acid Incorporated in a Poly(D,L-lactide) Implant Coating on Osteoblasts *in vitro*. *J. Biomed. Mater. Res., Part A* **2007**, *80*, 769–775.

(22) Bostman, O.; Pihlajamaki, H. Clinical Biocompatibility of Biodegradable Orthopaedic Implants for Internal Fixation: A Review. *Biomaterials* **2000**, *21*, 2615–2621.

(23) Garvin, K.; Feschuk, C. Polylactide-polyglycolide Antibiotic Implants. *Clin. Orthop. Relat. R.* **2005**, *437*, 105–110.

(24) Miyai, T.; Ito, A.; Tamazawa, G.; Matsuno, T.; Sogo, Y.; Nakamura, C.; Yamazaki, A.; Satoh, T. Antibiotic-loaded Poly-epsilon-caprolactone and Porous Beta-tricalcium Phosphate Composite for Treating Osteomyelitis. *Biomaterials* **2008**, *29*, 350–358.

(25) Rezwan, K.; Chen, Q. Z.; Blaker, J. J.; Boccaccini, A. R. Biodegradable and Bioactive Porous Polymer/Inorganic Composite Scaffolds for Bone Tissue Engineering. *Biomaterials* **2006**, *27*, 3413–3431.

(26) Zhu, M.; Zhang, L. X.; He, Q. J.; Zhao, J. J.; Guo, L. M.; Shi, J. L. Mesoporous Bioactive Glass-Coated Poly(L-lactic acid) Scaffolds: A Sustained Antibiotic Drug Release System for Bone Repairing. *J. Mater. Chem.* **2011**, *21*, 1064–1072.

(27) Zhu, Y. F.; Ikoma, T.; Hanagata, N.; Kaskel, S. Rattle-Type Fe₃O₄@SiO₂ Hollow Mesoporous Spheres as Carriers for Drug Delivery. *Small* **2010**, *6*, 471–478.

(28) Vallet-Regi, M.; Ramila, A.; del Real, R. P.; Perez-Pariente, J. A New Property of MCM-41: Drug Delivery System. *Chem. Mater.* **2001**, *13*, 308–311.

(29) Harmankaya, N.; Karlsson, J.; Palmquist, A.; Halvarsson, M.; Igawa, K.; Andersson, M.; Tengvall, P. Raloxifene and Alendronate Containing Thin Mesoporous Titanium Oxide Films Improve Implant Fixation to Bone. *Acta. Biomater.* **2013**, *9*, 7064–7073.

(30) Ehlert, N.; Badar, M.; Christel, A.; Lohmeier, S. J.; Luessenhop, T.; Stieve, M.; Lenarz, T.; Mueller, P. P.; Behrens, P. Mesoporous Silica Coatings for Controlled Release of the Antibiotic Ciprofloxacin from Implants. *J. Mater. Chem.* **2011**, *21*, 752–760.

(31) Ehlert, N.; Mueller, P. P.; Stieve, M.; Lenarz, T.; Behrens, P. Mesoporous Silica Films as a Novel Biomaterial: Applications in the Middle Ear. *Chem. Soc. Rev.* **2013**, *42*, 3847–3861.

(32) Wang, X. P.; Li, X.; Onuma, K.; Ito, A.; Sogo, Y.; Kosuge, K.; Oyane, A. Mesoporous Bioactive Glass Coatings on Stainless Steel for Enhanced Cell Activity, Cytoskeletal Organization and AsMg Immobilization. *J. Mater. Chem.* **2010**, *20*, 6437–6445.

(33) Brinker, C. J.; Lu, Y. F.; Sellinger, A.; Fan, H. Y. Evaporation-Induced Self-assembly: Nanostructures Made Easy. *Adv. Mater.* **1999**, *11*, 579.

(34) Karlsson, J.; Jimbo, R.; Fathali, H. M.; Schwartz, H. O.; Hayashi, M.; Halvarsson, M.; Wennerberg, A.; Andersson, M. *In vivo* Biomechanical Stability of Osseointegrating Mesoporous TiO₂ Implants. *Acta. Biomater.* **2012**, *8*, 4438–4446.

(35) Zhu, M.; Wang, H. X.; Liu, J. Y.; He, H. L.; Hua, X. G.; He, Q. J.; Zhang, L. X.; Ye, X. J.; Shi, J. L. A Mesoporous Silica Nanoparticulate/beta-TCP/BG Composite Drug Delivery System for Osteoarticular Tuberculosis Therapy. *Biomaterials* **2011**, *32*, 1986–1995.

(36) Takuma, A.; Kaneda, T.; Sato, T.; Ninomiya, S.; Kumegawa, M.; Hakeda, Y. Dexamethasone Enhances Osteoclast Formation Synergistically with Transforming Growth Factor-beta by Stimulating the Priming of Osteoclast Progenitors for Differentiation into Osteoclasts. *J. Biol. Chem.* **2003**, *278*, 44667–44674.

(37) Feng, S. M.; Deng, L. F.; Chen, W.; Shao, J. Z.; Xu, G. L.; Li, Y. P. Atp6v1c1 is An Essential Component of the Osteoclast Proton Pump and in F-actin Ring Formation in Osteoclasts. *Biochem. J.* **2009**, *417*, 195–203.

(38) Manzano, M.; Lamberti, G.; Galdi, I.; Vallet-Regi, M. Anti-Osteoporotic Drug Release from Ordered Mesoporous Bioceramics: Experiments and Modeling. *AAPS PharmSciTech.* **2011**, *12*, 1193–1199.

(39) Zhao, W. R.; Chen, H. R.; Li, Y. S.; Li, L.; Lang, M. D.; Shi, J. L. Uniform Rattle-type Hollow Magnetic Mesoporous Spheres as Drug Delivery Carriers and their Sustained-Release Property. *Adv. Funct. Mater.* **2008**, *18*, 2780–2788.

(40) Kienapfel, H.; Sprey, C.; Wilke, A.; Griss, P. Implant fixation by bone ingrowth. *J. Arthroplasty.* **1999**, *14*, 355–368.

(41) Kurth, A. H.; Eberhardt, C.; Muller, S.; Steinacker, M.; Schwarz, M.; Bauss, F. The Bisphosphonate Ibandronate Improves Implant Integration in Osteopenic Ovariectomized Rats. *Bone* **2005**, *37*, 204–210.

(42) Peter, B.; Pioletti, D. P.; Laib, S.; Bujoli, B.; Pilet, P.; Janvier, P.; Guicheux, J.; Zambelli, P. Y.; Bouler, J. M.; Gauthier, O. Calcium Phosphate Drug Delivery System: Influence of Local Zoledronate Release on Bone Implant Osteointegration. *Bone* **2005**, *36*, 52–60.

(43) Zhu, Y. F.; Shi, J. L.; Li, Y. S.; Chen, H. R.; Shen, W. H.; Dong, X. P. Hollow Mesoporous Spheres with Cubic Pore Network as a Potential Carrier for Drug Storage and Its in Vitro Release Kinetics. *J. Mater. Res.* **2005**, *20*, 54–61.